Evidence for fracture-hosted fluid-rock reactions within geothermal reservoirs of the eastern trans-Mexico volcanic belt

Chris Rochelle[1,*], Alicja Lacinska[1], Andrew Kilpatrick[1], Jeremy Rushton[1], Leandra M. Weydt[2], Kristian Bär[2] and Ingo Sass[2,3]

[1]British Geological Survey, Nicker Hill, Keyworth, Nottingham, NG12 5GG, UK

[2]Department of Geothermal Science and Technology, Technische Universität Darmstadt, Schnittspahnstraße 9, 64287 Darmstadt, Germany

[3]Darmstadt Graduate School of Excellence Energy Science and Engineering, Otto-Berndt-Straße 3, 64287 Darmstadt, Germany

*caro@bgs.ac.uk

ABSTRACT

Fractures within hydrothermal systems represent major pathways for fluid flow, and it is therefore vital that we understand processes occurring along them as these may have an impact on productivity of hot fluids during geothermal exploitation. This is especially important where hydrothermal activity crosses contrasting rock types, as fluid movement can result in a range of fluid-rock reactions, mineral dissolution and precipitation, and possible changes in fracture permeability.

Here we report evidence of fluid-rock reactions within basement carbonates and overlying volcanic rocks within hydrothermally altered rocks of the eastern trans-Mexico volcanic belt, as part of the Europe-Mexico collaborative 'GEMex' project (EU-H2020, GA No. 727550). Identified reactions within basement carbonates include initial high temperature Si-metasomatism linked to igneous intrusions to form minerals such as olivine, wollastonite, garnet and diopside, followed by subsequent lower temperature hydration (back reaction) at lower temperatures, where olivine and diopside hydrate to form serpentine and talc. Reactions of overlying andesitic units include Ca-metasomatism and bleaching through interaction of rising acidic, carbonate-equilibrated fluids. Secondary minerals produced during these reactions appear to seal fractures, implying tectonic reactivation of fractures to maintain long-term fluid flow through fracture zones.

1.INTRODUCTION

A vast amount of the presently accessible geothermal resource cannot be exploited with conventional technologies (Huenges, 2010). Such 'unconventional' resources include enhanced geothermal systems (EGS) in very hot environments (hot-EGS), and super-hot geothermal systems (SHGS) where deep geothermal fluids exceed temperatures of 350°C. To address the technical challenges associated with these systems (Kruszewski and Wittig, 2018), two sites in Mexico have been selected for detailed study as part of the collaborative European-Mexico GEMex project: the Acoculco (hot-EGS) and Los Humeros (SHGS) caldera complexes. Both sites are located in the northeastern part of the Trans-Mexican Volcanic Belt (TMVB) in Puebla. The GEMex project comprises a multidisciplinary approach integrating a large number of teams of researchers with wide-ranging methodologies (Bruhn, 2020; Jolie et al., 2018). The aim is to construct integrated reservoir models of the deep geothermal systems, and through a better understanding of such systems develop appropriate strategies for deep exploration and effective exploitation. The studies of the active geothermal sites at Acoculco (AC) and Los Humeros (LH) have been extended by parallel studies of ancient or fossil geothermal systems at Zacatlan and Las Minas (Veracruz State) (Liotta et al., 2020). At Las Minas exhumation and deep erosion has exposed fluid flow zones showing evidence for several, potentially analogous, generations of different fluid-rock reactions as the systems evolved along a decreasing temperature gradient. There is thus an opportunity to study and compare samples showing evidence of fluid-rock reactions occurring over a range of spatial and temporal scales. A good understanding of paleo or in-situ stress state and fracture orientations are key to understanding fluid movement within geothermal systems (Liotta, 2020), and as a consequence borehole flow rates and the power potential of geothermal plants. Fluid-rock reactions leading to mineral dissolution or precipitation along such fractures have the potential to alter fluid flow rates, and so it is important to understand the variety and extent of such reactions. Additionally, this is also important in terms of characterising reservoir petrophysical properties, resulting in direct input parameters for the reservoir models (Weydt et al., 2020). Here we report a selection of observations of samples from borehole core (active systems) and outcrop samples (exhumed analogue system) showing evidence of such reactions.

Both active and analogue systems are based around igneous heat sources, comprising intrusions into Jurassic-Cretaceous carbonates. The active systems at AC and LH comprise large calderas (Avellán et al., 2018; Carrasco-Núñez et al., 2018; Norini et al., 2015), within which a number of igneous heat sources are expected. At LH the oldest volcanic activity is represented by thick sequences of andesites, dacites, basalts and vitric tuffs (10.5 Ma until 1.55 Ma), which overlay the carbonate basement and form the presently-exploited geothermal reservoir (Carrasco-Núñez et al., 2018). The later emplacement of the LH caldera is associated with two main caldera-forming eruptions (Xaltipán ignimbrite at ca. 169 ka, and Zaragoza ignimbrite at ca. 69 ka), multiple voluminous plinian eruptions, as well as alternating episodes of dacitic and rhyodacitic dome-forming eruptions (Carrasco-Núñez et al., 2017). The succession of rocks in the Las Minas area is made up of Paleozoic granodiorite basement covered by a thick sequence of Cretaceous limestones, intruded by Tertiary (Miocene) dioritic to granitic rocks, and passing to a quaternary basalt and to dacitic to rhyolitic pyroclastites (see Liotta et al., 2020). The intrusions caused the development of a thick metamorphic contact aureole in the surrounding limestones, with the formation of marbles and associated metasomatic rocks - skarns (Ferriz and Mahood, 1984).

There is evidence of fracturing at a range of scales within the exposed rocks at Las Minas, and within borehole core from Los Humeros, and a variety of alteration mineralogy is found in and around these fractures. Fractures in the carbonates control the upward flow of hot fluids into the overlying andesitic rocks, and fluid movement along these fractures has resulted in a range of different fluid-rock reactions, mass transfer, and solids volume changes (ΔV). To better understand the variety and extent of near-fracture reactions and their relationships to structural features, we have analysed samples of borehole materials and outcrop samples. Here, we describe a small selection of the mineralogical changes observed, and frame them in terms of volume changes of solids and their potential to impact fluid flow along the fractures. More details about these and other samples are presented in Rochelle et al. (2019). To make our results more accessible, we reference these to a simplified, model of a granitic intrusion into limestone basement (Fig 1.) and illustrate the variety of different reactions, buy reference to specific evidence found in samples of borehole core, rock exposures, or experimental residues.
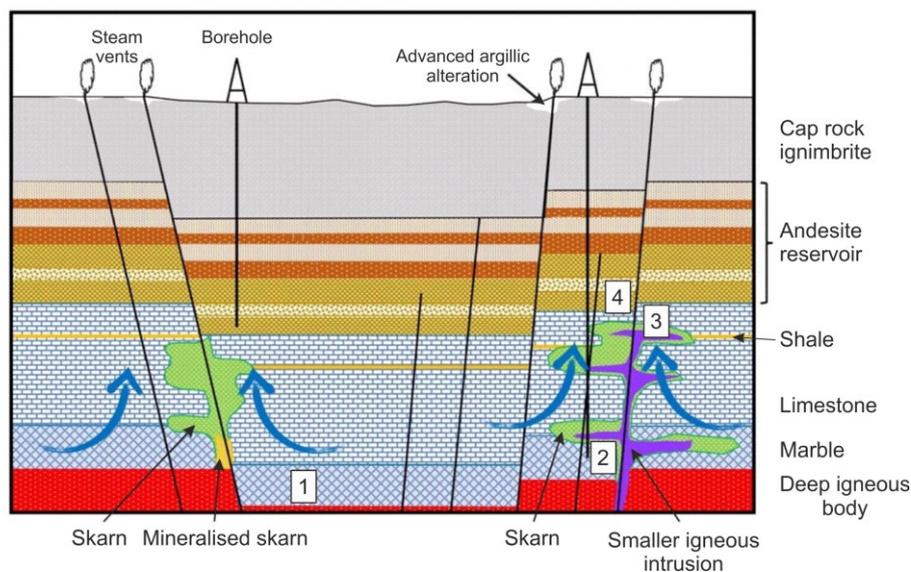

Figure 1: Schematic representation of key parts of a deep geothermal systems (not to scale) on the example of the Los Humeros geothermal field.

This work is part of the 'reservoir characterization' work group within the GEMex project (Jolie et al., 2018, Weydt et al., 2018) and provides a brief introduction into the types of fluid-rock reaction observed along fractures in the systems studied. It is part of ongoing studies and we continue to examine some of the samples, more details can be found in Rochelle et al. (2019) and Weydt et al. (2019a,b).

2. SAMPLES AND METHODOLOGY

Within the GEMex project, several joint field trips were conducted in order to identify the main fracture pattern (Liotta et al., 2019; Norini et al., 2019) geometry and distribution of geological units in the area. Also to characterize all key units from the basement to the cap rock in terms of their petrophysical and thermophysical rock properties (Weydt et al., 2018, 2020) and mineralogy (Rochelle et al., 2019) at different scales. In total more than 330 outcrop samples were collected for petrophysical and mineralogical investigations (Weydt et al., 2019a). Furthermore, 64 core samples covering 14 wells of the LH geothermal field were obtained (Weydt et al., 2019b).

Only a selection of the rock samples is described here, including thermally-altered carbonate (i.e. marble) samples known to be close to an igneous body from outcrops in the Las Minas area, and limestone and andesite samples from LH borehole core. The samples were prepared as polished thin sections 30 µm thick, which were studied by both optical microscope and scanning electron microscope (SEM). SEM was performed using an FEI Quanta 600 SEM with an Oxford Instruments X-Max detector (SDD) for Energy Dispersive Spectrometry (EDS), running with Oxford Instruments INCA (v4) software. The SEM was operated at: 20 kV accelerating voltage, approximately 5 nA beam current; and an acquisition time of 60 seconds per spot was used. EDS process time of 4 resulted in dead-times of <45%. Use of Backscattered SEM imaging (i.e. BSEM) aided phase identification, with EDS analysis providing quantification of phase compositions.

As well as study of natural materials, a few experimentally-produced samples (BGS Hydrothermal Laboratory) were also analysed. These were prepared by loading ca. 1 g granulated samples into gold capsules with a small amount of synthetic geothermal fluid. The capsules were welded shut, placed into autoclaves and subjected to elevated pressures and temperatures (500°C, 500 bar) simulating possible in-situ conditions. This was done to be able to compare reaction products from very well-controlled conditions, and also to get a first order indication of the rates of fluid-rock reactions. Characterisation of reaction products was via SEM as per the above, but samples were prepared as grain mounts on aluminium stubs.

3. FLUID-ROCK REACTIONS

The following descriptions aim to illustrate the variety of important fluid-rock reactions along fractures. These are not exhaustive, but serve to show the complexities of reactions within both the limestone basement (possible future SHGS reservoir) and the currently exploited geothermal reservoir. Reactions are described in order of decreasing temperature, such as might be experienced by a pulse of geothermal fluid migrating down a temperature gradient. However, there is also an element of time-dependency, as

the hottest reactions would only happen immediately after intrusion of the igneous material, whereas lower temperature reactions could continue for some considerable time. Lower temperature reactions are also expected to overprint earlier, higher temperature ones.

We note that dolomite is common at Las Minas, though was not observed in borehole core from LH, the lower parts of which are dominated by limestone. Depositional differences may account for the variation in abundance of dolomite, but the limited number of deep carbonate samples from the LH boreholes mean that we cannot rule out the possibility of dolomite at depth at LH. The presence of Mg-rich carbonates results in very different mineral alteration assemblages compared to Ca-rich carbonates, and it is useful to compare the differences in reactions that result.

3.1 Thermal metamorphism and rehydration of carbonate basement

Prior to the advection of geothermal fluids, igneous emplacement altered the nature of the host carbonates through thermal metamorphism (e.g. of approximately 800 °C in the case of granite), leading to dehydration and metamorphism of the carbonates, creating marble. There is evidence from Las Minas (Lacinska et al., 2018, 2019a) of abundant magnesium-rich carbonate in places (dolomitic limestone prior to heating), with metamorphism forming dolomite marble. Where heating was most severe, i.e. the immediate metamorphic contact aureole, dolomite ($CaMg(CO_3)_2$) broke down to calcite ($CaCO_3$) and periclase (MgO), forming periclase marble:

$$CaMg(CO_3)_2 \rightarrow CaCO_3 + MgO + CO_2 \quad (\Delta V \text{ approximately -25\%}) \tag{1}$$
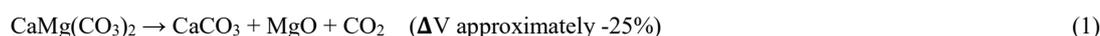
Progressive cooling of the rocks allowed influx of H_2O-rich fluids into the marble. Whilst calcite and remaining dolomite marble appear unaffected, periclase was hydrated (retrograde reaction) to form a brucite-rich ($Mg(OH)_2$) marble:

$$MgO + H_2O \rightarrow Mg(OH)_2 \quad (\Delta V \text{ approximately +45\%}) \tag{2}$$

The exact timing of this hydration is unclear, though the presence of veins of high temperature phases cutting brucite marble (see below) suggest that it was early in the sequence of events. The large change in volumes of the solids associated with the above reactions would have created fracturing at a range of scales, facilitating loss of CO_2 for reaction (1) and ingress of H_2O for reaction (2) Indeed, reaction (2) appears to have resulted in microfracturing around brucite grains (former grains of periclase, see Fig. 2) due to expansion during hydration.
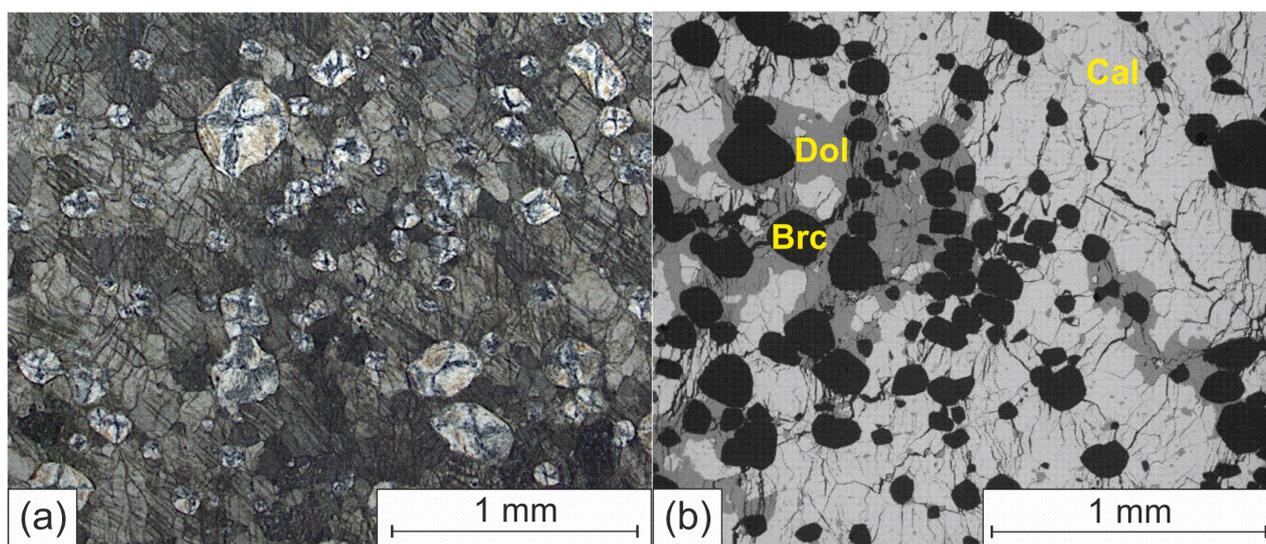

Figure 2: Optical photomicrograph of brucite crystals (typical 'onion skin') in calcite (a) and SEM image of brucite crystals (dark) with dolomite (grey) and fractured calcite (light) in (b).

3.2 Metasomatic reactions in carbonate basement

Si-rich fluids moved out of the setting magma body along faults and fractures in the carbonate basement. Morelli et al. (2018) suggest that for Las Minas these early fluids were hypersaline (>60 wt% NaCl) and at 550-600°C, and at a pressure of 1.8kbar. The migration of this fluid resulted in considerable reaction with, and metasomatism of, the host carbonates, and the formation of skarn bodies. Some of the fluids appear to have also carried metals such as iron, leading to skarns adjacent to the magma body being mineralised to economic concentrations (metallic mineralisation is outside the scope of this study). In the samples studied (which are inferred to be more distal from the magma body), it is evident that fracture-controlled metasomatism was the most common replacement mechanism within the carbonates. As fluid flow was focused along specific fracture-controlled flow paths, individual skarn bodies are relatively limited in size, however the high degree of reaction results in large changes in their chemical makeup, and hence also their petrophysical properties.

In many cases, the solids volume change upon fluid-rock reaction appears to have been sufficient to seal the fractures, thus time-limiting the extent of fluid flow along them. An implication of a tendency for fractures to self-seal, would be that long-term fluid

flow would require periodic reactivation of flow paths via tectonic processes. It is noteworthy therefore, that the evidence pointing to fracture reactivation is retrograde alteration of the initially high-temperature mineral assemblages by later, hydrothermal fluids (see later comments).

Metasomatic reactions in calcic marble and limestone

Metasomatic reactions led to skarn formation in calcic marble, which contains a range of calc-silicate minerals such as wollastonite (addition of Si), grossular-andradite garnet (addition of Si, Al, ± Fe), and locally also some diopside where Mg was added. This is seen in borehole core from LH (sample code H 13-3-x-C1, see Lacinska and Rochelle, 2019b), where a fine-grained and deformed calcite marble is cross-cut by an array of narrower (<200 μm wide) and thicker (up to 4 mm wide) veins (Fig. 3). The thickest veins are composed of coarse (up to 1 mm), interlocking calcite crystals. The thinner veins contain wollastonite, grossular and subordinate diopside, apatite and pyrite, often found in the central parts and interstitially intergrown with coarse calcite. Coarse crystals of recrystallised calcite were seen around some of the veins and associated with areas that appeared bleached in hand specimen. Wollastonite and grossular were also observed as interstitial domains within the host marble. When associated with wollastonite, the grossular occurs as irregular patches. In places, the grossular seems to have been partially replaced by wollastonite, but it is unclear if this represents the overall paragenetic sequence, or was just a local reaction.

Recrystallisation of $CaCO_3$ along the margins of the vein suggests ingress of a hot fluid saturated with $CaCO_3$. The reactions seen in finer veins are consistent with ingress of a hotter fluid rich in silica, and carrying some dissolved Fe, Al and Mg - as indicated by the presence of pyrite, grossular and diopside. Based on the evidence from other samples analysed in this study, the precipitation of silicates and sulphides is not concomitant, and the sulphides are inferred to represent a later stage in the evolution of the system. Precipitation of iron as pyrite suggests also that the fluid was reducing and contained some dissolved H_2S.
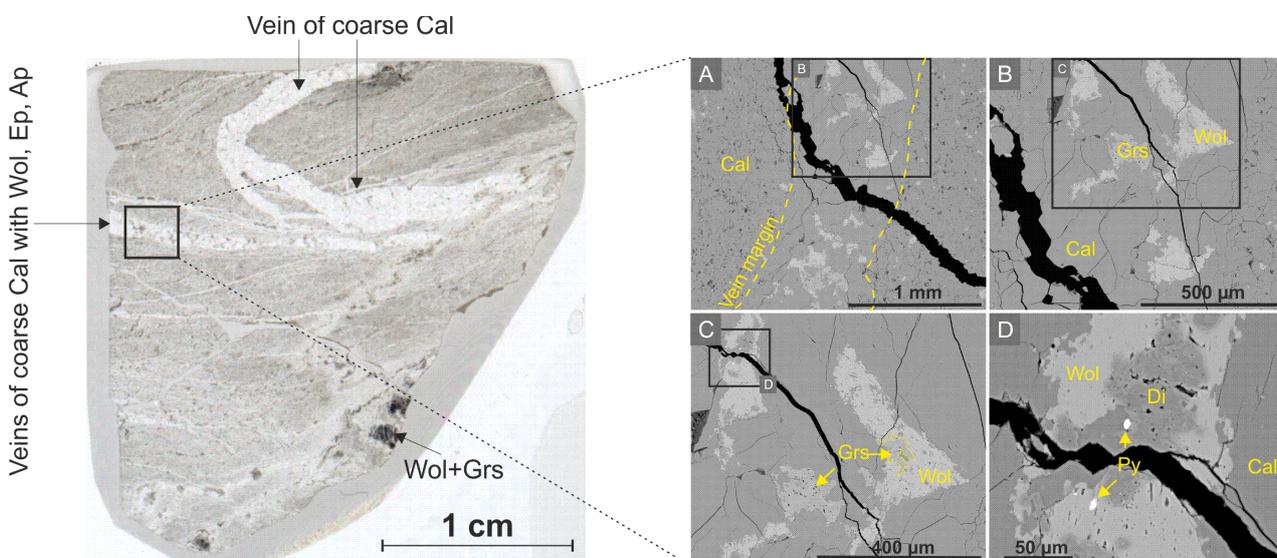

Figure 3: Scan of polished thin section of sample H13-3-x-C1 on the left and backscattered scanning electron microscopy images of wollastonite-grossular coarse calcite vein on the right, with subordinate diopside and pyrite (Wol = wollastonite, Grs = grossular, Cal = calcite, Di = diopside). Note the common presence of wollastonite along the vein margin.

Initially, the reaction between fluid and rock would have been fast, but the formation of layers of Ca(Al)-silicate phases (e.g. wollastonite) on fracture walls could inhibit reaction of Si from the superhot geothermal fluid with the host carbonate rock, and exchange of Ca from the rock into the geothermal fluid. Consequently, the 'armouring' (sealing) of fracture walls, would impact chemical mass transport, and facilitate continued advection of Si in the hydrothermal fluids. This would tend to increase the likelihood of finding Si-enriched fluids in fractures during the exploration of superhot systems in the carbonate basement.

Key reactions in terms of filling of the fracture space are the formation of wollastonite ($CaSiO_3$) from dissolved silica reacting with the marble:

$$CaCO_3 + SiO_2 => CaSiO_3 + CO_2 \quad (\Delta V \text{ approximately } +8\%) \tag{3}$$
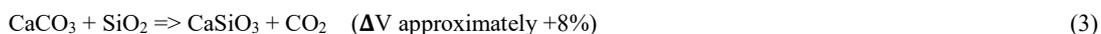
The formation of grossular ($Ca_3Al_2Si_3O_{12}$) required additional Al, which could have been sourced from the hydrothermal fluid or from the dissolution of phases such as clays that are known to be interspersed with the limestone locally (they have been observed in various outcrops of the Jurassic and Cretaceous limestones). In the former case:

$$3CaCO_3 + 3SiO_2 + 2Al^{3+} + 3H_2O => Ca_3Al_2Si_3O_{12} + 3CO_2 + 6H^+ \quad (\Delta V \text{ approximately } +13\%) \tag{4}$$
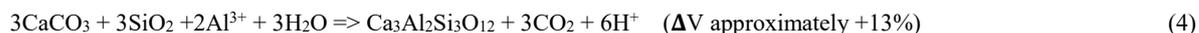
Both reactions release CO_2. In an open system this would migrate away as either a dissolved or free phase, and would tend to drive the reactions to produce more wollastonite and grossular.

That wollastonite can be formed very quickly was demonstrated in laboratory experiments reacting granulated limestone with quartz sand in gold capsules at 500°C and 500 bar for <2 weeks. 1 g of each solid was reacted with a simplified version of an acidic brine (consisting of 3M NaCl and 0.1% HCl). Quartz grains were almost completely dissolved, and limestone grains deeply etched, resulting in significant amounts of fibrous wollastonite (Fig. 4) (for more details see Rochelle et al., 2019).
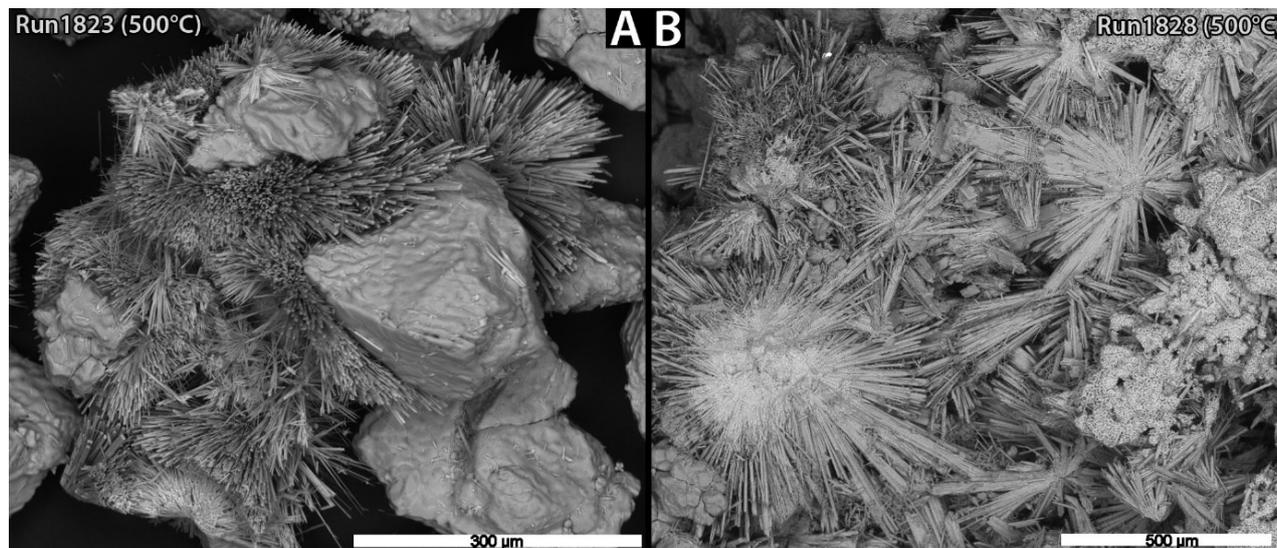

Figure 4: Backscattered SEM images, of grain mount samples of experimental reaction products. Note deeply etched and embayed limestone fragments cemented by abundant fibrous wollastonite. Only a very few remnants of sand grains were observed in these products. Run conditions: 500°C, 500 bar, Run 1823 = 2 weeks, Run 1828 = 1 week.

Whilst diopside ($CaMgSi_2O_6$) appeared as a minor phase in the borehole core limestone, it was more abundant in samples from Las Minas (presumably because of more Mg in the circulating fluids) (Fig. 5). This reaction produces a small decrease in solids volume of approximately 10%:

$$2CaCO_3 + 2SiO_{2(aq)} + Mg^{2+} => CaMgSi_2O_6 + Ca^{2+} + 2CO_2 \quad (\Delta V \text{ approximately } -10\%) \tag{5}$$
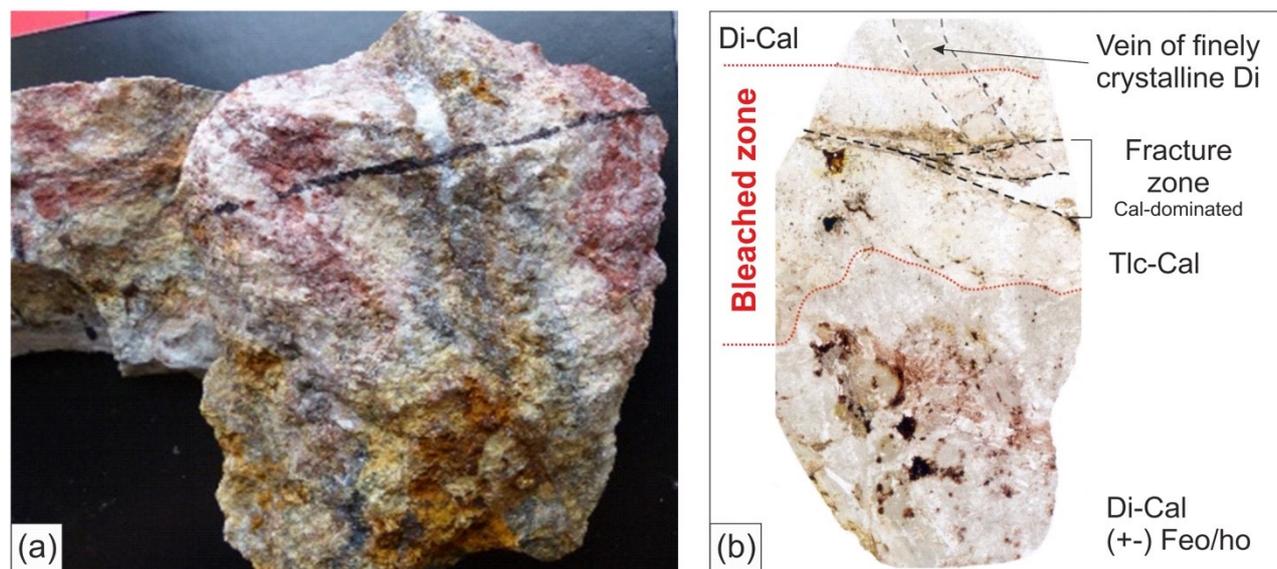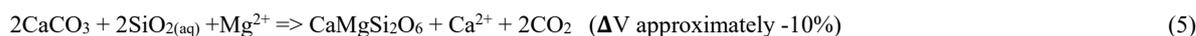

Figure 5: Fist-sized sample of veined calcic marble (a) and scan of a polished thin section of the sample (width 2.5 cm, in b). Note the presence of earlier formed diopside (Di) from the carbonate, and later formed talc (Tlc). High temperature fluids also appear to have caused bleaching of the rock. Calcite veining suggests that the sample may have undergone multiple fracturing events. Feo/ho represents Fe oxide/oxyhydroxide.

In the case of the limestone sample above, the low abundance of diopside would make the reduction in solids volume minor, and it would have been compensated for by the formation of garnet and wollastonite, both present in larger quantities. Subsequent lower temperature hydration of diopside formed talc ($Mg_3Si_4O_{10}(OH)_2$):

$$3CaMgSi_2O_6 + 6H^+ => Mg_3Si_4O_{10}(OH)_2 + 2SiO_2 + 3Ca^{2+} + 2H_2O \qquad (6)$$
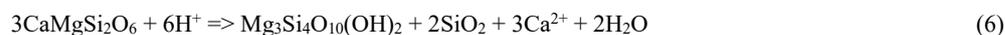
Overall therefore, the influx of hot, silica-rich fluids into fractured calcic marble led to the formation of secondary phases (wollastonite and grossular garnet) that will tend to seal fractures. Maintaining hydrothermal flow over long timescales would therefore appear to require tectonic processes to reactivate fractures, leading to later influx of hydrothermal fluids. Hydration of high temperature phases to form new (but weaker) minerals could result in changes in petrophysical properties compared to their anhydrous counterparts. If present in significant amounts, these secondary hydrated phases may affect overall rock petrophysical properties (e.g. locally lower rock strength) as described by Weydt et al. (2020).

Metasomatic reactions in Mg-rich marble

There is ample evidence of Mg carbonate and its transformation products in the samples from Las Minas. Although, the mechanism of metasomatic reactions in dolomitic and periclase/brucite marbles are similar to those in calcic protolith, the resultant mineral assemblage and skarn textures appear to be notably different. Mg-rich minerals such as forsterite and diopside (plus secondary serpentine and talc) and subordinate spinel minerals dominate the Mg-skarns, whereas Ca-rich phases such as wollastonite and garnet are rare or absent. As per the calcic skarns, alteration occurs along fracture surfaces, and also fills them. Under high temperature conditions, where silica-rich fluids can migrate into dolomite, then forsterite olivine (Mg_2SiO_4) and calcite form:

$$2CaMg(CO_3)_2 + SiO_2 => 2CaCO_3 + Mg_2SiO_4 + 2CO_2 \qquad (7)$$

Some samples from Las Minas showed evidence of metasomatic veins with stringers of <100 μm crystals of forsterite, as well as <400 μm aggregates, intergrown with calcite (see Lacinska and Rochelle, 2018). A minor amount of <50 μm crystals of diopside were also observed. The transformation of dolomite into calcite and forsterite is associated with a solids volume decrease of approximately 9%, which would potentially aid further fluid ingress.

The distinctive calcite + forsterite (in places later serpentine and talc formed during retrograde reactions) zoned veins, distinguishable on a scale of several micrometres to several centimetres around a central fracture suggest either: a) multiple, parallel fracturing events, with several stages of forsterite growth, or b) a single event, where the counter-diffusion of Si and Mg either side of a single fracture resulted in several (at least 3 in Fig. 6) zones of simultaneous forsterite precipitation - we continue to study the potential mechanisms of such diffusion-related phenomena.
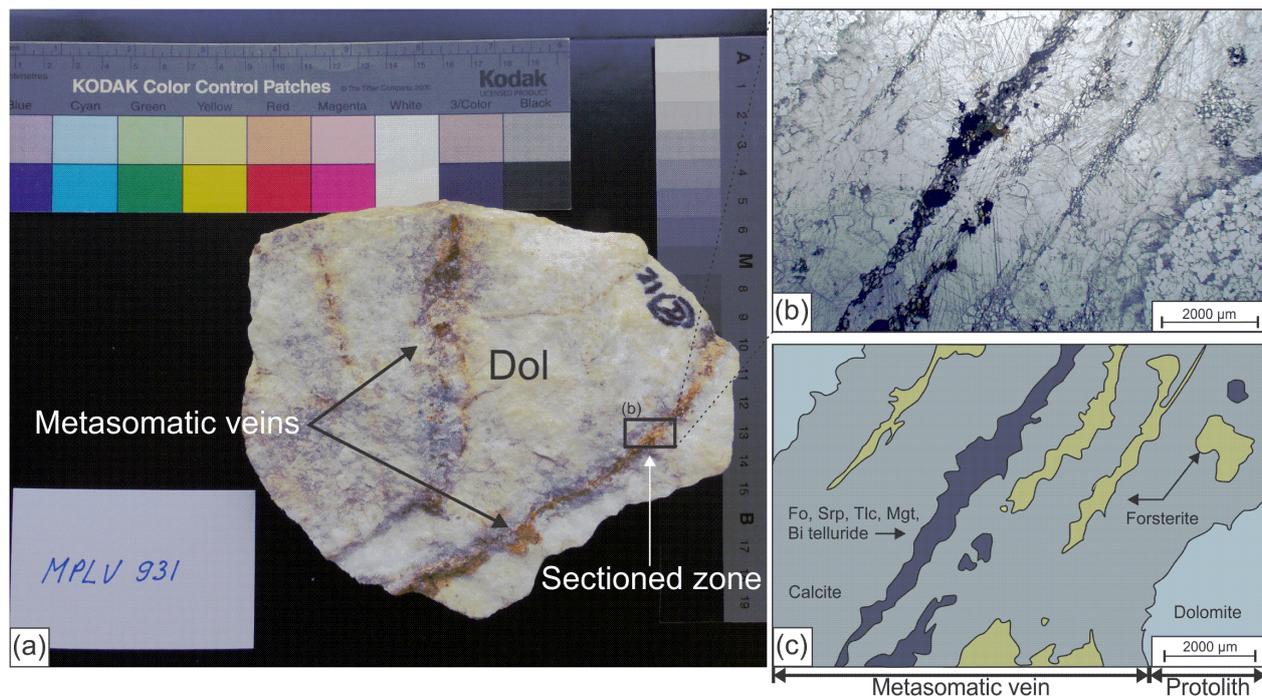

Figure 6: Metasomatic veins in dolomite (a). Forsterite and calcite replace original dolomite marble (b and c). Serpentine (Srp) and talc (Tlc) formed at later stage retrograde phases. Metallic mineralisation (magnetite, + trace Bi-, Cu-, Zn-, Pb-containing phases) is associated with the late hydrothermal event.

Other samples from closer to the granitic intrusion (i.e. where thermal metamorphism[2] was more severe) reveal evidence for silica reaction with periclase/brucite (these being secondary products of high temperature decarbonization of dolomite). It is unclear from the samples available if the metasomatic event was post-periclase hydration, or coeval with it. Our working hypothesis is of a

fracturing event allowing high temperature Si-rich fluid (± H_2O) into periclase/brucite marble. This recrystallised calcite at the fracture surfaces, and leached Mg from the wallrock to form a vein of forsteritic olivine within the fracture (reaction 8 and Fig. 7). Also formed were a range of spinels ($MgAl_2O_4$ and minor qandilite spinel [Mg, Fe^{2+}]$_2$[Ti, Fe^{3+}, Al]O_4).

$$2MgO + SiO_2 => Mg_2SiO_4 \qquad \text{and/or} \qquad 2Mg(OH)_2 + SiO_2 => Mg_2SiO_4 + 2H_2O \tag{8}$$

It is also evident that the initial high temperature metasomatic event has been overprinted by a later hydrothermal event, where forsterite was hydrated (back reacted) to serpentine minerals ($Mg_3Si_2O_5(OH)_4$) (9) and talc (10):

$$2Mg_2SiO_4 + 3H_2O => Mg_3Si_2O_5(OH)_4 + Mg(OH)_2 \tag{9}$$

$$4Mg_2SiO_4 + 6H_2O => Mg_3Si_4O_{10}(OH)_2 + 5Mg(OH)_2 \tag{10}$$
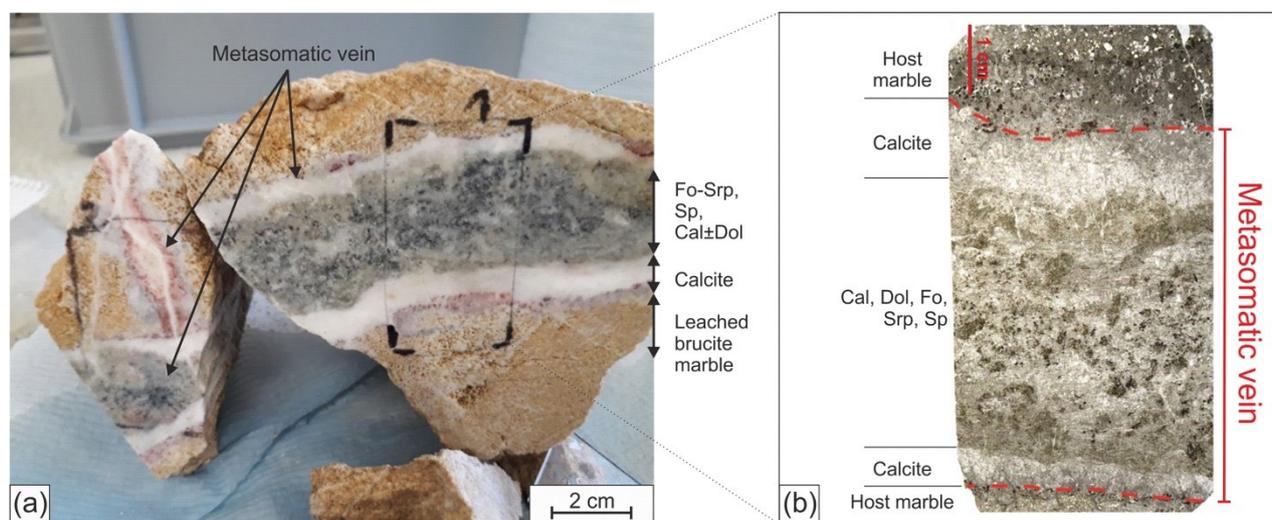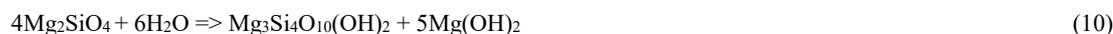

Figure 7: Fist-sized sample (a) with metasomatic veining. Leached brucite marble with mineralogically zoned vein (Fo = forsterite, Srp = serpentine, Sp = spinel, Cal = calcite, Dol = dolomite). Scan of a thin section across the vein (b).

The serpentinisation reaction has a potential volume increase of approximately 65% if all the original fosteritic olivine was hydrated. Whilst serpentinisation and talc formation might at first appear to be a mechanism to seal routes of water ingress (due to a solids volume increase), it is also possible that such a large solids volume increase could have led to microfracturing of the rock, locally or pervasively, aiding further water ingress. Further study is needed to estimate the extent of retrograde alteration along fractures

There is uncertainty about the timing of periclase hydration within the periclase/brucite marble (host rock for the fracture in Fig. 7). However, the associated 45% solids volume increase led to pervasive microfracturing around former grains of periclase in a zone of rock adjacent to the fracture. This microfracturing allowed access for later fluids to dissolve the brucite, leaving a porous and weakened rock either side of the partially serpentinised vein (Fig. 8). Field-based observations at Las Minas of (albeit limited) exposures with several roughly parallel fractures 2-5 cm wide, suggest the possibility of clustering of fractures - i.e. potentially signifying multiple fracturing events focused in one zone. Additionally, Mg sheet silicates such as serpentine and talc have significantly lower frictional strength than their anhydrous counterparts, potentially affecting the overall strength of the rock mass and its potential to move under tectonic forces (e.g. Moore and Rymer 2007). It is tentatively suggested therefore, that hydrothermally-altered skarns in dolomite/periclase marble have the potential to act as sites of stress relief via fracturing, and thus form a focus of fluid flow. Consequently, there could be geothermal exploitation benefits (in terms of enhanced fluid flow) in targeting skarns in dolomite/periclase marble in the carbonate basement.
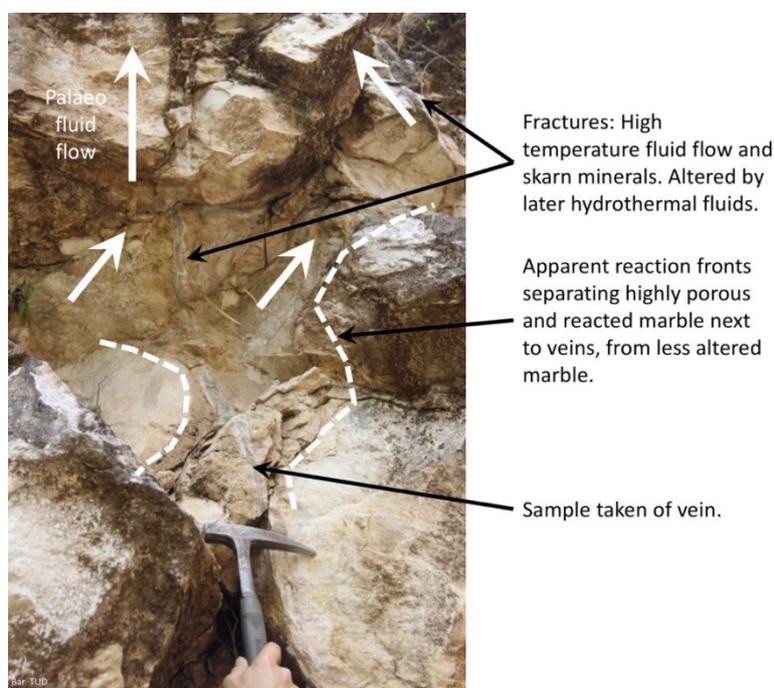
Figure 8: Exposed face of altered Mg-rich marble close to Las Minas. Note the alteration zone of crumbly rock adjacent to the filled fracture.

3.3 Reactions in andesitic reservoir rocks

Unlike the fracture-dominated permeability of the carbonate basement rocks, the andesitic reservoir rock possesses both matrix and fracture permeability (Weydt et al. [2018] and references therein). These will facilitate mixing and dilution of the (igneous-derived, acid gas rich) fluids from the carbonate basement with geothermal fluids in the andesitic reservoir. This difference in permeability will also increase contact between fluids and minerals enhancing the degree of reaction. Consequently, alteration of the andesites can be more pervasive (rather than limited to immediately adjacent to veins), and bulk rock physical properties are changed over a larger volume.

The andesites are also of a very different chemical composition to the underlying carbonates, and the types of fluid-mineral reactions will also change, largely due to the presence of a range of aluminosilicate minerals such as feldspars and pyroxenes, and also volcanic glass. Not only do these provide additional elements to incorporate into reactions, but their hydrolysis consumes acidity. The latter is important as it would turn an acidic, corrosive deep geothermal fluid into one with a more moderate pH.

To demonstrate the types of reactions occurring around fractures in andesitic rocks, we consider a sample of borehole core from LH that shows different features depending upon the position close to hydrothermal fluid upflow zones. The reactions observed are consistent with what we might expect for location [4] in Fig. 1.

The sample H38-4-25-C1 is from the lower part of the andesite (1950-1953 m) that serves as the currently-exploited geothermal reservoir. It is an altered volcanic rock (possibly a quartz-bearing andesite) with a matrix composed of plagioclase, K feldspar and quartz with subordinate titanite, apatite, pyrite, Fe oxide; and scattered < 1 mm phenocrysts of partially altered amphibole and K feldspar-plagioclase. The sample appears to be a fragment of a fracture zone within the andesite that served as pathway for fluids carrying components that have changed the rock chemistry in and around the fracture (Fig. 9). A notable reaction front formed in the wall rock. The apparent fracture zone (on the right in Fig. 9) is occupied by $\leq$ 5 mm euhedral to subhedral crystals of garnet (andradite composition) intergrown with elongate and blocky crystals of calcite. The garnets are rich in < 200 μm mineral inclusions, of which pyroxene (diopside-augite composition) dominates, with lesser amounts of calcite, chlorite, pyrite and acicular wollastonite. Acicular wollastonite was also observed on the crystals of garnets, intergrown with calcite. Calcite appears to be the latest phase formed in the fracture.

With increasing distance into the wallrock and away from the fracture there are a series of zones with different mineralogy:

- Fracture to 0.5 cm: Epidote + calcite + chlorite + garnet, with volcanic textures largely overprinted by the alteration including significant dissolution as manifested by notable secondary porosity and euhedral crystals of epidote.

- 0.5 to 1.5 cm: Dominantly epidote-replaced volcanic rock with subordinate titanite and amphibole. This zone contains numerous moderately porous, $\leq$ 2 mm wide epidote and calcite + epidote (+ minor chlorite) veins.

- 1.5 cm onwards: Locally bleached and altered volcanic rock. The alteration encompasses localised formation of epidote and chlorite, both partially replacing the rock matrix and the scattered phenocrysts of amphibole and plagioclase.

The presence of andradite garnet, wollastonite and calcite in the inferred fracture suggest significant influx of Ca (Ca metasomatism) into the relatively low-Ca andesitic lithology (Ca metasomatism). The presence of the mineral assemblage typical of skarns within andesite is unusual. The Ca (plus associated CO_2 and other acidic gases) likely originated from underlying marble/limestone and was carried by the ascending hydrothermal fluid. Two possible, (slightly contrasting) conclusions result from this observation. Firstly, that fluid-rock reaction had not yet had time to reduce the concentration of Ca in the fluid, and as such, likely came from a location relatively close to the limestone/andesite contact. Secondly, the presence of significant Ca-rich secondary phases on fracture walls might have acted to 'armour' (seal) them from further reaction. The presence of garnets at the contact between limestone and andesite is also reported nearby, with Lieber and Frenzel (2003) reporting the presence of green garnet in pockets at the contact between limestone and andesite below the amethyst area of Piedra Parada, north of Las Minas.
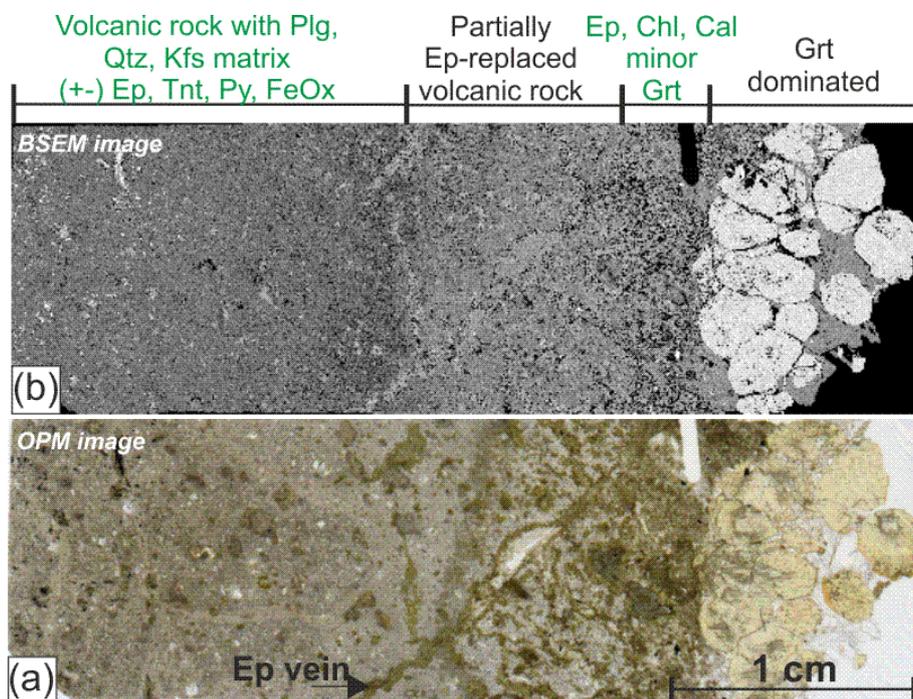

Figure 9: Backscattered electron image (b) and a scan (transmitted light) of the whole polished thin section (a), with Grt = garnet, Ep = Epidote, Chl = chlorite, Tnt = titanite, Py = pyrite, Cal = calcite.

Dissolution of the andesite wallrock by a (presumed) acidic hydrothermal fluid led to leaching of a range of elements, including Si, Al and Fe. The leaching of Fe from Fe oxide/hydroxide led to bleaching of the wallrock. The release of Si and Fe, followed by their diffusion towards the fracture, would allow andradite garnet ($Ca_3Fe_2Si_3O_{12}$) to grow upon the reaction with the (presumed) relatively Ca-rich hydrothermal fluid. The euhedral and coarse morphology of the garnets and calcite suggest a relatively open fracture at the time these phases grew (though continued growth of them would potentially seal the fracture). We have no direct evidence to say whether or not bulk rock properties were improved or degraded as a result of these reactions. However, based just on the evidence of significant dissolution, we suggest that rock strength was reduced, and this continues to be investigated.

The Al released from aluminosilicate (e.g. plagioclase) dissolution was available for the formation of epidote in either vein, or wallrock. Reactions for the anorthite end-member component of plagioclase reacting without / in the presence of Fe to form (a) Fe-free epidote or (b) Fe-rich epidote, are:

a) $\quad 3CaAl_2Si_2O_8 + Ca^{2+} + 2H_2O => 2Ca_2Al_3Si_3O_{12}(OH) + 2H^+$ $\hfill$ (11)

b) $\quad 8CaAl_2Si_2O_8 + 8Ca^{2+} + 8Fe^{2+} + 8SiO_2 + 22H_2O + CO_2 => 8Ca_2FeAl_2Si_3O_{12}(OH) + 32H^+ + CH_4$ $\hfill$ (12)
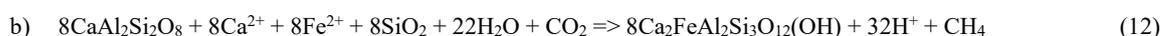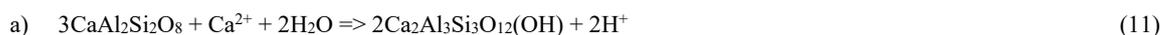
In the case of the latter reaction, this would result in a solids volume increase of 38%, which would aid vein sealing. The potential for oxidation of Fe^{II} to Fe^{III} to reduce CO_2 to methane is also noted. This reaction is only tentatively proposed as we have no direct evidence for CO_2 reduction to methane at LH. However, we note that some of the natural surface gas releases being monitored at LH contain small amounts of methane (GEMex work under Task 4.3, Taylor pers. comm.).

Rochelle et al.

4. CONCLUSIONS AND OUTLOOK

We report observations of fluid-rock reactions associated with fractures in both carbonate and volcanic rocks found within the eastern Trans-Mexican Volcanic Belt. This work is done as part of Europe-Mexico collaboration within the joint GEMex project, and ongoing work investigates the impact of the observed processes on rock properties. The reactions studied are relevant to 'superhot' (>350°C) conditions within the very deep roots of hydrothermal systems where igneous bodies have intruded basement limestones, and at shallower levels where volcanic rocks host the presently-exploited geothermal fluids (such as at Los Humeros). Exploiting such systems will be critically-dependent on sustaining sufficiently-high flow rates of geothermal fluids, so intersecting fractures during drilling is vital. Fluid-rock reactions along such fractures can influence both fluid chemistry and fracture as well as rock properties, so it is important to understand these in detail to understand and predict long-term reservoir behaviour. Samples representing deep, fractured carbonates were obtained from a deeply-eroded fossil geothermal system around the town of Las Minas, which is being studied as an analogous system to Los Humeros (i.e. a natural analogue). Samples of altered volcanic material (andesite) and recrystallized limestone were retrieved from borehole cores from the Los Humeros geothermal system.

Intrusion of igneous material into basement carbonates produced a metamorphic contact aureole, with limestone and dolomite being converted to marble. Fractures through the marble and more distal non-metamorphosed carbonates allowed very high temperature Si-rich (±Al, Fe) fluids to migrate away from the igneous body, resulting in Si-metasomatism of the carbonates and the formation of skarns. The skarn minerals were initially anhydrous, and include olivine at highest temperatures, plus also wollastonite, garnet and diopside (the latter requiring Mg, either from the fluid or a Mg-rich host rock). Though the formation of these phases at the surfaces of fractures consumed some of the Si from the superhot fluids, there is potential for sealing of their surfaces against further fluid-rock reactions. For high flow rate conditions, this potentially may facilitate further movement of Si-enriched geothermal fluids. Whilst the migration of Si-enriched superhot geothermal fluids may cause issues in their exploitation (e.g. silica scale formation within boreholes and surface infrastructure), the fact that they may be saturated with phases such as wollastonite and garnet may at least allow for better prediction of fluid chemistry using predictive geochemical codes.

Where the superhot fluids migrated into the overlying andesite rocks (e.g. the current production zone at Los Humeros), their high dissolved Ca content caused (localized) Ca-metasomatism of the silicate rock, and the formation of a wollastonite/garnet/epidote assemblage typical of a skarn. Bleaching of the andesite around the fractures suggests that these fluids were acidic, driven by H^+ ions diffusing into the wallrock. Acid-driven dissolution of minerals in the wallrock created significant secondary porosity and released Fe - which back-diffused towards the fracture and reacted with H_2S in the geothermal fluids to precipitate pyrite. The andesitic rocks are thus important for neutralization of acidity, and formation of a less aggressive geothermal fluid.

The formation of secondary minerals within fractures would act to seal them, and so longer-term fluid movement requires periodic reactivation of the fractures (likely due to tectonically-driven activity of the still active caldera system). We see evidence for this, with some introducing H_2O-rich hydrothermal fluids into previously high-temperature zones within carbonate basement. These fluids hydrated the original anhydrous phases, converting olivine and diopside to serpentine minerals and talc. Again, these reactions also acted to seal fractures, and the hydrated secondary phases may have different petrophysical properties to the original minerals, possibly facilitating future movement along the fractures. Thus maintaining long-term fluid flow within fracture zones in these hydrothermal systems likely requires multiple episodes of tectonically-driven fracturing, leading to some of the complexities observed in the samples studied.

REFERENCES

Bruhn, D.: GEMex – cooperation in geothermal energy research Europe-Mexico for development of enhanced geothermal systems and superhot geothermal systems, *Proceedings*, World Geothermal Congress 2020, Reykjavik, Iceland, Reykjavik, Iceland, April 26 – May 2, 2020, this volume.

Carrasco-Núñez, G., Bernal, J. P., Dávilla, P., Jicha, B., Giordano, G. and Hernández, J.: Reappraisal of Los Humeros Volcanic Complex by New U/Th Zircon and 40Ar/39Ar Dating: Implications for Greater Geothermal Potential, *Geochemistry, Geophysics, Geosystems*, 19, doi: 10.1002/2017GC007044, (2018), 132-149.

Carrasco-Núñez, G., Hernández, J., De Léon, L., Dávilla, P., Norini, G., Bernal, J. P., Jicha, B., Jicha, B., Navarro, M., and López-Quiroz, P.: Geologic Map of Los Humeros volcanic complex and geothermal field eastern Trans-Mexican Volcanic Belt, *terra digitalis*, **1**, (2017), 1-11.

Ferriz, H. and Mahood, G.: Eruptive rates and compositional trends at Los Humeros volcanic center, Puebla, Mexico, *Journal of Geophysical Research*, 89, (1984), 8511-8524.

Huenges, E.: Geothermische Stromerzeugung – Grundstrom für den erneuerbaren Energiemix 2050, FVEE Themen 2010, 73– 76, 2010, in: Tagungsband 2010: Forschung für das Zeitalter der erneuerbaren Energien, Forschungs Verbund Erneuerbare Energien, *Renewable Energy Research Association*, Berlin, Germany, (2010), p. 148.

Jolie, E., Bruhn, D., López Hernández, A., Liotta, D., Garduño-Monroy, V. H., Lelli, M., Páll Hersir, G., Arango-Galván, C., Bonté, D., Calcagno, P., Deb, P., Clauser, C., Peters, E., Hernández Ochoa, A. F., Huenges, E., González Acevedo, Z. I., Kieling, K., Trumpy, E., Vargas, J., Gutiérrez-Negrín, L. C., Aragón-Aguilar, A., Halldórsdóttir, S., González Partida, E., van Wees, J.-D., Ramírez Montes, M. A., Diez León, H. D., and the GEMex team: GEMex – A Mexican-European Research Cooperation on Development of Superhot and Engineered Geothermal Systems, *Proceedings*, 43rd Workshop on Geothermal Reservoir Engineering Stanford University, Stanford, California, February 12-14, 2018, SGP-TR-2013, (2018), p. 10.

Lacinska A.M. and Rochelle, C.A.: Petrographic description of a deformed marble cross-cut by metasomatic veins. Off-cut from core H 13-3-x-c1, depth 1200-1203 m. BGS sample MPLW 136, *British Geological Survey,* Report OR/19/008, (2019b).

Lacinska A.M., Rochelle, C.A. and Kemp, S.J.: Petrographic description of selected samples of skarns from the exhumed system of Las Minas, *British Geological Survey*, Report OR/19/007, (2019a)

Lacinska, A.M. and Rochelle, C.A.: Chapter 7: High temperature metasomatic veins and retrograde alteration, in 'WP4.1 – final report on understanding from exhumed systems, Deliverable D4.2, WP4, GEMex H2020 project, *European Comission*, **1**, http://www.gemex-h2020.eu, (2018), 260-289.

Lieber, W. and Frenzel, G.: Famous mineral localities: Las Vigas, Veracruz, Mexico. *The Mineralogical Record*, **34(6)**, (2003), 55-91.

Liotta, D., Bastesen, E., Bianco, C., Brogi, A., Caggianelli, A., Monroy, V. H. G., Partida, E. G., Haro, A. J., Kozdroj, W., Laurenzi, M., Morelli, G., Nawrocki, J., Garcia, E. O., Nawrocka, M. P., Rochelle, C. A., Ruggieri, G., Torabi, A., Wheeler, W., and Zucchi, M.: Analogue Geothermal Systems in Mexico: insights from the Deep Part of Los Humeros Geothermal Field in the Las Minas Mining Area (Eastern Mexico), *Proceedings*, World Geothermal Congress 2020, Reykjavik, Iceland, April 26 – May 2, 2020, (2020), this volume.

Liotta, D., Brogi, A., Garduño-Monroy, V. H., Gomez, F., Wheeler, W. H., Bastesen, E., Torabi, A., Bianco, C., Jimenez-Haro, A., Olvera-Garcia, E., Zucchi, E.: Regional Geological Structures, in: Final report on active systems: Los Humeros and Acoculco, Deliverable 4.1, WP4, GEMex H2020 project, *European Comission*, **1**, http://www.gemex-h2020.eu, (2019), 293-304.

Moore, D.E. and Rymer, M.J.:Talc-bearing serpentinite and the creeping section of the San Andreas Fault. Nature, **448**, (2007), 795-797.

Morelli, G., Zucchi, M., Ruggieri, G., Ventruti, G. and Partida, E.G.: Chapter 6: fluid inclusion studies and radiogenic and stable isotope analyses. In GEMex report 'WP4.1 – final report on understanding from exhumed systems – Deliverable D4.2' WP4, GEMex H2020 project, *European Comission*, **1**, http://www.gemex-h2020.eu, (2018), 222-259.

Norini, G. Gropelli, G., Sulpizio, R., Carrasco-Núñez, G., Dávila-Harris, P., Pellicioli, C., Zucca, F., and De Franco, R.: Structural analysis and thermal remote sensing of the Los Humeros Volcanic Complex: Implications for volcano structure and geothermal exploration, *Journal of Volcanology and Geothermal Research*, **301**, (2015), 221-237.

Norini, G., Carrasco–Núñez, G., Bonini, M., Montanari, D., Corti, G., and Moratti, G.: Geological Structures from Outcrops and Boreholes, in: Final report on active systems: Los Humeros and Acoculco, Deliverable 4.1, WP4, GEMex H2020 project, *European Comission*, **1**, http://www.gemex-h2020.eu, (2019), 54-77.

Rochelle, C., Kilpatrick, A., Lacinska, A. and Kemp, S.: Chapter 4.6: Evidence for fluid-rock reactions, in Bär, K. and Weydt, L. (2019): Comprehensive report on the rock and fluid samples and their physical properties in the Acoculco and Los Homeros regions, Deliverable D6.1, WP6, GEMex H2020 project, *European Comission*, **1.5**, http://www.gemex-h2020.eu, (2019), 112-159.

Rushton, J.C., Wagner, D., Pearce, J.M., Rochelle, C.A. and Purser, G. (in press): Red-bed bleaching in a CO_2 storage analogue: Insights from Entrada Sandstone fracture-hosted mineralization. Accepted for publication in the *Journal of Sedimentary Research*.

Weydt, L. M., Bär, K., and Sass, I.: Petrophysical reservoir characterization of the Los Humeros and Acoculco geothermal fields, Mexico, *Proceedings*, World Geothermal Congress 2020, Reykjavik, Iceland, April 26 – May 2, 2020, this volume.

Weydt, L. M., Bär, K., Colombero, C., Comina, C., Deb, P., Lepillier, B., Mandrone, G., Milsch, H., Rochelle, C. A., Vagnon, F., and Sass, I.: Outcrop analogue study to determine reservoir properties of the Los Humeros and Acoculco geothermal fields, Mexico, *Adv. Geosci.*, **45**, https://doi.org/10.5194/adgeo-45-281-2018, (2018), 281-287.

Weydt, L. M.: Chapter 1.3: Field work, sample distribution and classification, in Bär, K. and Weydt, L. (2019): Comprehensive report on the rock and fluid samples and their physical properties in the Acoculco and Los Humeros regions, Deliverable D6.1, WP6, GEMex H2020 project, *European Comission*, **1.5**, http://www.gemex-h2020.eu, (2019a), 7-14.

Weydt, L. M.: Chapter 2.1: Samples of Los Humeros Geothermal Field and Outcrop Analogues, in Bär, K. and Weydt, L. (2019): Comprehensive report on the rock and fluid samples and their physical properties in the Acoculco and Los Humeros regions, Deliverable D6.1, WP6, GEMex H2020 project, *European Comission*, **1.5**, http://www.gemex-h2020.eu, (2019b), 15-25.